Asymptotic Preserving Semi-Lagrangian Discontinuous Galerkin Methods for Multiscale Kinetic Transport Equations

Yi CAI

School of Mathematical Sciences

Xiamen University

Joint work with Tao Xiong (USTC),
Guoliang Zhang (SJTU), Hongqiang Zhu (NJUPT)

Beijing, PR China

June 15, 2024

Outline

Outline

1. Introduction
2. Characteristic-based model reformulation
3. Semi-Lagrangian discontinuous Galerkin method
4. Numerical results
5. Conclusion and future work

Mathematical model

Kinetic transport equation:

$$\partial_t f + v \cdot \nabla_x f = \mathcal{Q}(f). \tag{1}$$

- distribution function $f(t, x, v)$;
- time $t \in \mathbb{R}$; position $x \in \Omega_x \subset \mathbb{R}^d$; velocity $v \in \Omega_v \subset \mathbb{R}^d$;
- collision operator $\mathcal{Q}(f)$.

A diffusive scaling $t = t'/\varepsilon^2$, $x = x'/\varepsilon$ gives

$$\partial_t f + \frac{1}{\varepsilon} v \cdot \nabla_x f = \frac{1}{\varepsilon^2} \mathcal{Q}(f). \tag{2}$$

- Knudsen number $\varepsilon > 0$;
- ε is close to zero, diffusive regime; ε is away from zero, kinetic regime.

Collision operators

Let $(\Omega_v, \mathscr{F}_v, \mu)$ be a measure space, where $\Omega_v \subset \mathbb{R}^d$ is bounded and symmetric with respect to $\mathbf{0} \in \mathbb{R}^d$, $\mathscr{F}_v$ is a σ-algebra over Ω_v, μ is a probability measure such that $\int_{\Omega_v} 1 \, \mathrm{d}\mu = 1$. Assume $f(v) \in L^2(\Omega_v; \mathrm{d}\mu)$ and define $\langle f \rangle := \int_{\Omega_v} f(v) \, \mathrm{d}\mu$.

Examples of collision operators.

- Two-velocity models [Jang et al. 2015, JCP].
  Let $\Omega_v = \{-1, 1\}$ and $\mathrm{d}\mu$ discrete uniform measure, define

$$\mathcal{Q}(f) = \langle f \rangle - f; \tag{3a}$$

$$\mathcal{Q}(f) = \langle f \rangle - f + A\varepsilon v \langle f \rangle, \quad |A\varepsilon| < 1; \tag{3b}$$

$$\mathcal{Q}(f) = \langle f \rangle - f + C\varepsilon v[\langle f \rangle^2 - (\langle f \rangle - f)^2], \quad C > 0. \tag{3c}$$

$$\mathcal{Q}(f) = K \langle f \rangle^m (\langle f \rangle - f), \quad K > 0, \quad m \leq 0; \tag{3d}$$

- Linear transport equation. Let $\Omega_v = \mathbb{S}^{d-1}$ and $\mathrm{d}\mu = \frac{1}{|\mathbb{S}^{d-1}|} \mathrm{d}v$, define

$$\mathcal{Q}(f) = \sigma_s(\langle f \rangle - f) - \varepsilon^2 \sigma_a f + \varepsilon^2 S, \tag{4}$$

Diffusive limits

Let $\rho = \langle f \rangle$ and $\varepsilon \to 0$, we get $f \to \rho$ and

- models with collision (3a)-(3d) become

$$\partial_t \rho = \partial_{xx} \rho, \qquad \text{heat equation;} \tag{5a}$$

$$\partial_t \rho + A \partial_x \rho = \partial_{xx} \rho, \qquad \text{advection-diffusion equation;} \tag{5b}$$

$$\partial_t \rho + C \partial_x (\rho^2) = \partial_{xx} \rho, \qquad \text{viscous Burgers equation;} \tag{5c}$$

$$\partial_t \rho = (K(1-m))^{-1} \partial_{xx} (\rho^{1-m}), \qquad \text{porous media equation;} \tag{5d}$$

- model with collision (4) goes to

$$\partial_t \rho = \nabla_x \cdot (\langle v \otimes v \rangle \nabla_x \rho / \sigma_s) - \sigma_a \rho + S, \tag{6}$$

where $\otimes$ is the Kronecker product.

Numerical challenges

Difficulties.

- asymptotic preserving: capture the right diffusive limit as $\varepsilon \to 0$;
- multi-dimension: $x \in \mathbb{R}^3$, $v \in \mathbb{S}^2$.
- multi-scale: stiff both in streaming and collision;

Existing AP schemes.

- fully explicit schemes[1]: strict time step condition $\Delta t = O(\varepsilon h)$;
- fully implicit schemes[2]: solving a large-scale linear system is expensive.
- implicit-explicit schemes:
  - explicit diffusion[3]: $\Delta t = O(\varepsilon h + h^2)$;
  - implicit diffusion but explicit convection[4]: unconditionally stable if $\varepsilon \le \lambda h$ (diffusive regime) and otherwise $\Delta t = O(\frac{\varepsilon^2}{\varepsilon/h-\lambda})$ (kinetic regime).

[1] Jin 1995, JCP; Caflisch, Jin, and Russo 1997, SINUM
[2] Klar 1998, SINUM; Klar and Unterreiter 2002, SINUM
[3] Lemou and Mieussens 2008, SISC; Jang et al. 2015, JCP; Jang et al. 2014, SINUM
[4] Peng, Cheng, et al. 2020, JCP; Peng, Cheng, et al. 2021, SINUM; Peng and Li 2021, SISC

Research aims

Our aims.

- asymptotic preserving;
- uniformly unconditionally stable;
- only solve a small number of a small-scale linear system;
- weak formulation;
- friendly for parallel computing.

Preliminary work.

- Zhang, Zhu, and Xiong 2023, SISC;
- A family of asymptotic preserving uniformly unconditionally stable finite difference methods using a characteristic-based model reformulation.

Outline

Characteristic-based reformulation

Consider a multi-dimensional linear transport equation with a diffusive scaling:

$$\partial_t f + \tilde{v} \cdot \nabla_x f = \tilde{\sigma}(\rho - f). \tag{7}$$

where $\rho = \langle f \rangle$, $\tilde{v} = v/\varepsilon$ and $\tilde{\sigma} = \sigma/\varepsilon^2$ is a constant. The action of $\langle \cdot \rangle$ on (7) gives

$$\partial_t \rho + \nabla_x \cdot \langle \tilde{v} f \rangle = 0. \tag{8}$$

Main idea of constructing an AP scheme.

- Rewrite $F = \langle \tilde{v} f \rangle$ to be of form $G = G(f_{old}, \nabla_x \rho)$.
- The known data f_{old} is obtained by tracking along characteristics of (7) from a target time level t to an old time level t'.
- When a discrete ordinate method is applied, we focus on the discrete data $\{f(v_\alpha)\}$ over a finite set of velocities $\{v_\alpha\}$, and estimate the action of operator $\langle \cdot \rangle$ via a weighted summation, i.e., $\langle f(v) \rangle \approx \sum_\alpha w_\alpha f(v_\alpha)$.

Derivation: formal solution

Characteristic form. Let $x \in \Omega_x$ and $t > 0$ be given. By the chain rule of calculus, we get

$$\frac{\mathrm{d} f_v}{\mathrm{d} s}(s) = \tilde{\sigma}(\rho_v(s) - f_v(s)), \quad \frac{\mathrm{d}\xi_v}{\mathrm{d} s}(s) = \tilde{v}, \tag{9}$$

where $f_v(s) = f(s, \xi_v(s; x, t), v)$ and $\rho_v(s) = \rho(s, \xi_v(s; x, t))$ with $v \in \Omega_v$.

Formal solution. Given $0 \leq t' < t$, we get by exponential integration

$$f_v(t) = e^{-\tilde{\sigma}(t-t')} f_v(t') + \int_{t'}^{t} \tilde{\sigma} e^{-\tilde{\sigma}(t-s)} \rho_v(s) \, \mathrm{d}s, \tag{10a}$$

$$\xi_v(s; x, t) = x - \tilde{v}(t - s). \tag{10b}$$

Partial integration gives

$$f_v(t) = \rho_v(t) + e^{-\tilde{\sigma}(t-t')}(f_v(t') - \rho_v(t')) - \int_{t'}^{t} e^{-\tilde{\sigma}(t-s)} \frac{\mathrm{d}\rho_v}{\mathrm{d}s}(s) \, \mathrm{d}s. \tag{11}$$

Derivation: flux approximation

Approximated formal solution. With the following integral approximation,

$$\int_{t'}^{t} e^{-\tilde{\sigma}(t-s)} \frac{\mathrm{d}\rho_v}{\mathrm{d}s}(s)\,\mathrm{d}s \approx \int_{t'}^{t} e^{-\tilde{\sigma}(t-s)}\,\mathrm{d}s \frac{\mathrm{d}\rho_v}{\mathrm{d}s}(t) = \tilde{\sigma}^{-1}(1-e^{-\tilde{\sigma}(t-t')}) \frac{\mathrm{d}\rho_v}{\mathrm{d}s}(t).$$

we derived from (11) that

$$f_v(t) = \rho_v(t) + e^{-\tilde{\sigma}(t-t')}(f_v(t') - \rho_v(t')) - \tilde{\sigma}^{-1}(1-e^{-\tilde{\sigma}(t-t')}) \frac{\mathrm{d}\rho_v}{\mathrm{d}s}(t). \tag{12}$$

Approximated flux. Observe $\frac{\mathrm{d}\rho_v}{\mathrm{d}s}(t) = (\partial_t + \tilde{v}\cdot\nabla_x)\rho_v(t)$ and $\rho_v(t) = \rho(t,x)$. Insert (12) into $F = \langle \tilde{v} f\rangle$ with $\langle j(v)\rangle = 0$ for all odd functions $j(v)$, we get $F(t) \approx G(t,t')$ where

$$G(t,t') = \underbrace{e^{-\tilde{\sigma}(t-t')}\langle \tilde{v}(f(t') - \rho(t'))\rangle}_{\text{convection}} - \underbrace{(1-e^{-\tilde{\sigma}(t-t')})\tilde{\sigma}^{-1}\langle \tilde{v}\otimes\tilde{v}\rangle \nabla_x \rho(t)}_{\text{diffusion}}. \tag{13}$$

Model approximation: strong form

We define an SL operator $\mathcal{S}_v(t')$ that maps a function $g(t,x,v)$ to another function $g(t',\xi_v(t';x,t),v)$, i.e.,

$$\mathcal{S}_v(t')[g](t,x,v) = g(t',\xi_v(t';x,t),v), \quad \xi_v(t';x,t) = x - \tilde{v}(t-t'). \tag{14}$$

Assume a time domain $[0,T]$ and a equidistant partition $t^n = n\Delta t$ $(0 \le n \le N)$ with $\Delta t = T/N$, we set $t' = t^n$ and denote $\mathcal{S}_v^n = \mathcal{S}_v(t^n)$ for short.

Model approximation in a strong form. Let $f = \rho + \varepsilon g$ with $\langle g \rangle = 0$ and then $\tilde{v}(f-\rho) = vg$. With the flux approximation (13) and $\tilde{\sigma}^{-1}\langle \tilde{v} \otimes \tilde{v} \rangle = \sigma^{-1}\langle v \otimes v \rangle$, we get an approximated (ρ, f)-transport system: $\omega(t) = \exp(-\sigma(t-t^n)/\varepsilon^2)$

$$\partial_t \rho + \omega(t) \nabla_x \cdot \langle v \mathcal{S}_v^n[g] \rangle = \nabla_x \cdot \left((1-\omega(t)) \langle v \otimes v \rangle \nabla_x \rho / \sigma \right), \tag{15a}$$

$$\partial_t f + \frac{1}{\varepsilon} v \cdot \nabla_x f = \frac{\sigma}{\varepsilon^2}(\rho - f), \tag{15b}$$

As $\varepsilon \to 0$, we have $\omega(t) \to 0$ and (15) goes to the correct diffusive limit

$$f = \rho, \quad \partial_t \rho = \nabla_x \cdot \left(\langle v \otimes v \rangle \nabla_x \rho / \sigma \right). \tag{16}$$

Model approximation: weak form

Let K be an element of a spatial mesh $\mathcal{T}_h$ and denote $K(t)$ as a dynamic element obtained by tracing K along characteristics of f equation from t^{n+1} to t. Denote $\mathcal{D}_x$ as the differential operator in a weak sense.

Step 1. For ρ equation (15a), multiply with $\phi(x) \in L^2(\Omega_x)$ and integrate over an element $K \subset \Omega_x$, we get

$$\begin{aligned}\frac{\mathrm{d}}{\mathrm{d}t}\int_K \rho(t,x)\phi(x)\,\mathrm{d}x = &-\int_K \omega(t)\left\langle v\cdot\mathcal{D}_x\mathcal{S}_v^n[g](t,x,v)\right\rangle\phi(x)\,\mathrm{d}x \\ &+\int_K (1-\omega(t))\mathcal{D}_x\cdot\left(\langle v\otimes v\rangle\,\mathcal{D}_x\rho(t,x)/\sigma\right)\phi(x)\,\mathrm{d}x.\end{aligned} \tag{17}$$

Step 2. For f equation (15b), define a test function $\Psi(t,x)$ subject to

$$\partial_t\Psi(t,x) + \frac{1}{\varepsilon}v\cdot\nabla_x\Psi(t,x) = 0, \quad \Psi(t^{n+1},x) = \psi(x), \quad \forall\psi(x)\in L^2(\Omega_x). \tag{18}$$

By Reynold's transport theorem and divergence theorem, we get

$$\frac{\mathrm{d}}{\mathrm{d}t}\int_{K(t)} f(t,x,v)\Psi(t,x)\ \mathrm{d}x = \int_{K(t)} \frac{\sigma}{\varepsilon^2}(\rho(t,x)-f(t,x,v))\Psi(t,x)\ \mathrm{d}x. \tag{19}$$

Error estimate in model approximation

Theorem (Error estimate for flux approximation)

Let $0 < \varepsilon \leq 1$, $s \in [t', t]$ *and* $\Delta t = t - t'$. *Suppose that there exists a uniform upper bound* $M > 0$ *such that for all* $k \geq 1$ *and* $s \in [t, t']$,

$$\left|(\varepsilon \partial_t + v \cdot \nabla_x)^{k+1} \rho(s)\right| \leq M. \tag{20}$$

Then, the following error estimate holds for the flux approximation (13)*:*

$$\|F(t) - G(t, t')\|_\infty \leq C W^*(\varepsilon, \Delta t), \quad W^*(\varepsilon, \Delta t) = \begin{cases} \frac{\Delta t^2}{2\varepsilon^3}, & \text{if } \Delta t \leq \varepsilon^2; \\ \frac{\varepsilon}{1-\varepsilon}, & \text{if } \Delta t > \varepsilon^2, \end{cases} \tag{21}$$

where $C > 0$ *is a constant independent of* ε *and* Δt *but depends on* M *and velocity space* Ω_v.

Outline

Compact weak form with a consistent constraint

First order differential system. Define an auxiliary variable $q = \langle v \otimes v \rangle \mathcal{D}_x \rho / \sigma$. We add a consistent constraint $\rho = \langle f \rangle$ to formulate a $(\tilde{q}, \tilde{\rho}, f, \rho)$-system:

$$(\tilde{q}, \varphi)_K = \langle v \otimes v \rangle \ (\mathcal{D}_x \tilde{\rho}/\sigma, \varphi), \tag{22a}$$

$$\frac{\mathsf{d}}{\mathsf{d}t} (\tilde{\rho}, \phi)_K = -(\omega \langle v \mathcal{D}_x \mathcal{S}_v^n[g] \rangle, \phi) + ((1-\omega)\mathcal{D}_x \tilde{q}, \phi), \tag{22b}$$

$$\frac{\mathsf{d}}{\mathsf{d}t} (f, \Psi)_{K(t)} = \frac{1}{\varepsilon^2} (\sigma(\tilde{\rho} - f), \Psi)_{K(t)}, \tag{22c}$$

$$(\rho, \gamma)_K = (\langle f \rangle, \gamma)_K, \tag{22d}$$

for all $\varphi(x), \phi(x), \gamma(x) \in L^2(\Omega_x)$ and $\Psi(t, x)$ satisfies an adjoint problem (18) with $\Psi(t^{n+1}, x) = \psi(x) \in L^2(\Omega_x)$. Herein, $(\xi, \zeta)_K = \int_K \xi \zeta \, \mathsf{d}x$. As $\varepsilon \to 0$, we see that $\rho = \langle f \rangle = \tilde{\rho}$ holds in a weak sense.

Spatial discretization

Discontinuous finite element space. Given a quasi-uniform mesh $\mathcal{T}_h$ of size h with a boundary Γ_h, namely,

$$h \le c_0 r, \quad h = \max_{K\in\mathcal{T}_h} h_K, \quad r = \max_{K\in\mathcal{T}_h} r_K, \tag{23a}$$

$$h_K = \mathrm{diam}(K), \quad r_K = \max\left\{\mathrm{diam}(S)\,;\, S \text{ is a ball contained in } K\right\}. \tag{23b}$$

Solution spaces:

$$U_h^k = \left\{u \in L^2(\Omega_x)\,;\, u\big|_K \in \mathcal{P}^k(K), \quad \forall K \in \mathcal{T}_h\right\}; \tag{24}$$

$$V_h^k = \left\{u(\cdot, v) \in U_h^k\,;\, \int_{\Omega_v}\int_{\Omega_x} |u(x,v)|^2 dxdv < \infty\right\}. \tag{25}$$

Jump and average at a cell interface along a normal direction:

$$[\![u]\!](x) = u(x^+) - u(x^-), \quad \{\!\{u\}\!\}(x) = \frac{1}{2}\left[u(x^+) + u(x^-)\right]. \tag{26}$$

Spatial discretization

Semi-discrete scheme. Let $\tilde{q}_h, \tilde{\rho}_h, \rho_h \in U_h^k$ and $f_h, g_h = (f_h - \rho_h)/\varepsilon \in V_h^k$,

$$(\tilde{q}_h, \varphi)_K = \langle v \otimes v \rangle \, r_K(\tilde{\rho}_h/\sigma, \varphi), \tag{27a}$$

$$\frac{\mathsf{d}}{\mathsf{d}t} (\tilde{\rho}_h, \phi)_K = -b_K(\omega \langle v \mathcal{S}_v^n[g_h] \rangle, \phi) + l_K((1-\omega)\tilde{q}_h, \phi), \tag{27b}$$

$$\frac{\mathsf{d}}{\mathsf{d}t} (f_h, \psi)_{K(t)} = \frac{1}{\varepsilon^2} (\sigma(\tilde{\rho}_h - f_h), \psi)_{K(t)}, \tag{27c}$$

$$(\rho_h, \gamma)_K = (\langle f_h \rangle, \gamma)_K, \tag{27d}$$

where

$$r_K(\rho, \varphi) = \sum_{e \in \partial K} \int_e n_{e,K} \breve{\rho}_{e,K} \, \varphi \, \mathsf{d}\Gamma - \int_K \rho \nabla_x \varphi \, \mathsf{d}x, \tag{28a}$$

$$l_K(q, \phi) = \sum_{e \in \partial K} \int_e n_{e,K} \cdot \hat{q}_{e,K} \, \phi \, \mathsf{d}\Gamma - \int_K q \cdot \nabla_x \phi \, \mathsf{d}x, \tag{28b}$$

$$b_K(\langle v \mathcal{S}_v^n[g] \rangle, \phi) = \sum_{e \in \partial K} \int_e n_{e,K} \cdot \widetilde{\langle v \mathcal{S}_v^n[g] \rangle}_{e,K} \, \phi \, \mathsf{d}\Gamma - \int_K \langle v \mathcal{S}_v^n[g] \rangle \cdot \nabla_x \phi \, \mathsf{d}x. \tag{28c}$$

Spatial discretization

Diffusion fluxes:

$$\text{alternating left-right:}\quad \breve{\rho}_{e,K}(x) = \rho(x^-),\quad \hat{q}_{e,K}(x) = q(x^+); \tag{29a}$$

$$\text{alternating right-left:}\quad \breve{\rho}_{e,K}(x) = \rho(x^+),\quad \hat{q}_{e,K}(x) = q(x^-); \tag{29b}$$

$$\text{central:}\quad \breve{\rho}_{e,K}(x) = \frac{1}{2}\left[\rho(x^-) + \rho(x^+)\right],\quad \hat{q}_{e,K}(x) = \frac{1}{2}\left[q(x^-) + q(x^+)\right]. \tag{29c}$$

Upwind flux:

$$(\widetilde{vg})_{e,K}(x) = v\{\!\{g\}\!\} - \frac{|v|}{2}[\![g]\!] = \begin{cases} v\, g(x^+), & v \cdot n_{e,K} > 0; \\ v\, g(x^-), & v \cdot n_{e,K} < 0; \end{cases} \tag{30}$$

Temporal discretization

First order SL-LDG scheme. Let $\Delta t = t^{n+1} - t^n$ and then $\omega = e^{-\sigma \Delta t/\varepsilon^2}$. Apply backward Euler discretization to both $\tilde{\rho}$ and f equations, we get

$$(\tilde{q}_h^{n+1}, \varphi)_K = \langle v \otimes v \rangle \, r_K(\tilde{\rho}_h^{n+1}/\sigma, \varphi), \tag{31a}$$

$$(\frac{\tilde{\rho}_h^{n+1} - \rho_h^n}{\Delta t}, \phi)_K = -b_K(\omega \langle v \mathcal{S}_v^n[g_h] \rangle, \phi) + l_K((1-\omega)\tilde{q}_h^{n+1}, \phi), \tag{31b}$$

$$(f_h^{n+1}, \psi)_K = (\frac{\varepsilon^2}{\varepsilon^2 + \sigma\Delta t} f_h^n, \Psi^n)_{K^n} + (\frac{\sigma \Delta t}{\varepsilon^2 + \sigma \Delta t}\tilde{\rho}_h^{n+1}, \psi)_K, \tag{31c}$$

$$(\rho_h^{n+1}, \gamma)_K = (\langle f_h^{n+1} \rangle, \gamma)_K. \tag{31d}$$

Note that $(f, \Psi^n)_{K^n} = \int_K \mathcal{S}_v^n[f]\psi \, \mathrm{d}x$, which can be evaluated as the volume integral part of $b_K(\cdot, \cdot)$.

Temporal discretization

Second order SL-LDG scheme. Apply BDF2 method to $\tilde{\rho}$ equation and Crank-Nicolson method to f equations, we get

$$(\tilde{q}_h^{n+1}, \varphi)_K = \langle v \otimes v \rangle \; r_K(\tilde{\rho}_h^{n+1}/\sigma, \varphi), \tag{32a}$$

$$(\frac{\tilde{\rho}_h^{n+1} - 4\rho_h^n + 3\rho_h^{n-1}}{3\Delta t}, \phi)_K = -b_K(\omega \left\langle v\mathcal{S}_v^n[g_h] \right\rangle, \phi) + l_K((1-\omega)\tilde{q}_h^{n+1}, \phi), \tag{32b}$$

$$\begin{aligned}(f_h^{n+1}, \psi)_K =& (\frac{2\varepsilon^2}{2\varepsilon^2 + \sigma\Delta t} f_h^n, \Psi^n)_{K^n} + (\frac{\sigma\Delta t}{2\varepsilon^2 + \sigma\Delta t}\tilde{\rho}_h^{n+1}, \psi)_K \\ & - (\frac{\sigma\Delta t}{2\varepsilon^2 + \sigma\Delta t}(f_h^n - \rho_h^n), \psi)_{K^n},\end{aligned} \tag{32c}$$

$$(\rho_h^{n+1}, \gamma)_K = (\left\langle f_h^{n+1} \right\rangle, \gamma)_K. \tag{32d}$$

Oscillation-free damping approach

To control the numerical oscillation, we add a damping term to the f-equation.

$$\frac{\mathsf{d}}{\mathsf{d}t}\int_{K(t)} f_h \Psi \,\mathsf{d}x = \int_{K(t)} \frac{\sigma}{\varepsilon^2}(\tilde{\rho}_h - f_h)\Psi \,\mathsf{d}x - \sum_{l=0}^{k} \frac{\lambda_K^l(t^n)}{h_K} \int_{K(t)} (f_h - \pi_h^{l-1} f_h)\Psi \,\mathsf{d}x, \tag{33}$$

where $\pi_h^{-1} = \pi_h^0$ and π_h^l, $l \geq 0$, is a standard $L^2(\Omega_x)$ projection onto V_h^l, that is, for any function w, $\pi_h^l w \in V_h^l$ satisfies

$$\int_K (\pi_h^l w - w) v_h \,\mathsf{d}x = 0, \quad \forall v_h \in \mathcal{P}^l(K); \tag{34}$$

The damping coefficient is defined as

$$\lambda_K^l(t) = \frac{2(2l+1)}{2k-1} \frac{h^l}{l!} \sum_{|\alpha|=l} \left(\frac{1}{N_e} [\![\partial^\alpha f(t)]\!]^2 \right)^{\frac{1}{2}}. \tag{35}$$

Formal asymptotic analysis

Theorem

Assume that the telegraph equation (2)(3a) *is equipped with a periodic boundary condition and a well-posed initial condition. For a fixed time step* Δt *and mesh size* h*, as* $\varepsilon \to 0$*, the SL-LDG-*p*-*q *methods (*$p = 1, 2$*,* $q \geq 1$*) are formally AP.*

Fourier analysis

Consider the telegraph equation, take the ansatz

$$\boldsymbol{\rho}_i^n = \widehat{\boldsymbol{\rho}}^n \exp(\mathcal{I}\kappa x_i), \quad \boldsymbol{f}_{i,\alpha}^n = \widehat{\boldsymbol{f}}_\alpha^n \exp(\mathcal{I}\kappa x_i) \tag{36}$$

with $\mathcal{I}^2 = -1$ for $\alpha = -.+$. Let

$$\boldsymbol{U}_1^n = (\hat{\tilde{\boldsymbol{\rho}}}^n, \hat{\boldsymbol{f}}_-^n, \hat{\boldsymbol{f}}_+^n, \hat{\boldsymbol{\rho}}^n)^T, \quad \boldsymbol{U}_2^n = (\hat{\tilde{\boldsymbol{\rho}}}^n, \hat{\boldsymbol{f}}_-^n, \hat{\boldsymbol{f}}_+^n, \hat{\boldsymbol{\rho}}^n, \hat{\boldsymbol{\rho}}^{n-1})^T, \tag{37}$$

The SL-LDG-p-q methods is equivalent to:

$$\boldsymbol{U}_p^{n+1} = \boldsymbol{A}^{p,q}(\varepsilon, h, \Delta t; \omega)\boldsymbol{U}_p^n. \tag{38}$$

Principle for Numerical Stability: For any given $\varepsilon, h, \Delta t$, let the eigenvalues of amplification matrix $\boldsymbol{A}$ be $\lambda_i(\omega)$, $i = 1, \ldots, N$. Our scheme is "stable", if for all discrete wave number $\omega \in [0, 2\pi]$, it satisfies either

$$\max_{i=1,\ldots,N} \{|\lambda_i(\omega)|\} < 1, \quad \text{or} \tag{39a}$$

$$\max_{i=1,\ldots,N} \{|\lambda_i(\omega)|\} = 1 \quad \text{and} \quad \boldsymbol{A} \text{ is diagonalizable.} \tag{39b}$$

Fourier analysis

Theorem

For any given $q \geq 1$ and $p = 1, 2$, the amplification matrix $\boldsymbol{A}^{p,q}$ related to SL-LDG-p-q method depends only on $\frac{\varepsilon}{h}$ and $\frac{\Delta t}{\varepsilon h}$, namely, $\boldsymbol{A}^{p,q} = \boldsymbol{A}^{p,q}(\frac{\varepsilon}{h}, \frac{\Delta t}{\varepsilon h}; \omega)$.

Let $\sigma = \log_{10}(\varepsilon/h)$ and $\eta = \log_{10}(\varepsilon^2/\Delta t)$. We uniformly sample σ using 1000 points within $[-5, 5]$, and η with 800 points inside $[-4, 4]$. Additionally, we sample the discrete wave number ω uniformly within $[0, 2\pi]$ using 500 points. Based on the proposed stability principle, the SL-LDG-p-q methods with $p = 1, 2$ and $q = 1, 2$ are uniformly unconditionally stable.

Outline

1D telegraph equation: accuracy test

Let $\Omega_x = [-\pi, \pi]$, $\Omega_v = \{-1, 1\}$; $\varepsilon = 0.5, 10^{-1}, 10^{-2}, 10^{-6}$; $T = 1$;
Exact solution:

$$\begin{aligned} f(t,x,v) &= \frac{1}{4}\left[-\frac{1}{\gamma}e^{-\gamma t}\sin(x) + v\varepsilon e^{-\gamma t}\cos(x)\right] + \frac{1}{2}, \\ \rho(t,x) &= -\frac{1}{4\gamma}e^{-\gamma t}\sin(x) + \frac{1}{2}, \quad \gamma = \frac{2}{1+\sqrt{1-4\varepsilon^2}}. \end{aligned} \tag{40}$$

L^r-norms, $r = 1, \infty$:

$$E^{\rho}_{N,r} = \|\rho_h(T,x) - \rho(T,x)\|_{L^r}, \quad O^{\rho}_{N,r} = \log_2(E^{\rho}_{N,r}/E^{\rho}_{2N,r}), \tag{41}$$

1D telegraph equation: accuracy test

Table: Accuracy test for 1D telegraph equation. Numerical errors and convergence orders of the SL-LDG-1 method in L^1 and L^∞ norms. $T = 1$.

Parameters		$\Delta t = 0.5h$				$\Delta t = 5.0h$			
ε	N	$E^\rho_{N,1}$	$O^\rho_{N,1}$	$E^\rho_{N,\infty}$	$O^\rho_{N,\infty}$	$E^\rho_{N,1}$	$O^\rho_{N,1}$	$E^\rho_{N,\infty}$	$O^\rho_{N,\infty}$
0.5	80	1.59E-02	-	4.48E-03	-	1.38E-01	-	3.46E-02	-
	160	7.61E-03	1.06	2.18E-03	1.04	8.01E-02	0.79	2.00E-02	0.79
	320	3.73E-03	1.03	1.08E-03	1.02	3.51E-02	1.19	8.80E-03	1.19
	640	1.85E-03	1.01	5.35E-04	1.01	1.42E-02	1.31	3.55E-03	1.31
10^{-1}	80	1.43E-02	-	4.68E-03	-	6.05E-02	-	1.54E-02	-
	160	9.11E-03	0.65	2.86E-03	0.71	3.72E-02	0.70	9.43E-03	0.71
	320	4.96E-03	0.88	1.63E-03	0.81	2.10E-02	0.83	5.30E-03	0.83
	640	2.37E-03	1.07	8.59E-04	0.93	1.30E-02	0.69	3.28E-03	0.69
10^{-2}	80	1.08E-02	-	4.05E-03	-	5.75E-02	-	1.47E-02	-
	160	5.39E-03	1.00	2.02E-03	1.00	3.32E-02	0.79	8.44E-03	0.80
	320	2.70E-03	1.00	1.01E-03	1.00	1.73E-02	0.94	4.38E-03	0.95
	640	1.36E-03	0.99	5.07E-04	1.00	8.85E-03	0.96	2.24E-03	0.97
10^{-6}	80	1.07E-02	-	4.05E-03	-	5.75E-02	-	1.47E-02	-
	160	5.36E-03	1.00	2.02E-03	1.00	3.32E-02	0.79	8.43E-03	0.80
	320	2.68E-03	1.00	1.01E-03	1.00	1.72E-02	0.94	4.37E-03	0.95
	640	1.34E-03	1.00	5.02E-04	1.00	8.81E-03	0.97	2.23E-03	0.97

1D telegraph equation: accuracy test

Table: Accuracy test for 1D telegraph equation. Numerical errors and convergence orders of the SL-LDG-2 method in L^1 and L^∞ norms. $T = 1$.

Parameters		$\Delta t = 0.5h$				$\Delta t = 5.0h$			
ε	N	$E^{\rho}_{N,1}$	$O^{\rho}_{N,1}$	$E^{\rho}_{N,\infty}$	$O^{\rho}_{N,\infty}$	$E^{\rho}_{N,1}$	$O^{\rho}_{N,1}$	$E^{\rho}_{N,\infty}$	$O^{\rho}_{N,\infty}$
0.5	80	2.37E-03	-	6.12E-04	-	1.04E-01	-	2.60E-02	-
	160	6.14E-04	1.95	1.58E-04	1.95	4.36E-02	1.25	1.09E-02	1.25
	320	1.56E-04	1.98	4.00E-05	1.98	1.34E-02	1.70	3.35E-03	1.70
	640	3.92E-05	1.99	1.01E-05	1.99	3.65E-03	1.87	9.13E-04	1.88
10^{-1}	80	4.04E-03	-	1.10E-03	-	3.49E-02	-	8.81E-03	-
	160	3.07E-03	0.40	7.91E-04	0.48	1.08E-02	1.68	2.73E-03	1.69
	320	1.53E-03	1.00	3.89E-04	1.02	5.21E-03	1.06	1.31E-03	1.06
	640	5.57E-04	1.46	1.41E-04	1.47	4.17E-03	0.32	1.04E-03	0.33
10^{-2}	80	2.81E-04	-	1.64E-04	-	3.15E-02	-	7.98E-03	-
	160	9.67E-05	1.54	4.75E-05	1.78	7.34E-03	2.10	1.86E-03	2.10
	320	5.17E-05	0.90	1.87E-05	1.34	1.66E-03	2.14	4.21E-04	2.14
	640	4.05E-05	0.35	1.16E-05	0.69	4.23E-04	1.97	1.07E-04	1.97
10^{-6}	80	2.45E-04	-	1.54E-04	-	3.15E-02	-	7.97E-03	-
	160	5.99E-05	2.03	3.83E-05	2.01	7.30E-03	2.11	1.85E-03	2.11
	320	1.49E-05	2.01	9.55E-06	2.00	1.62E-03	2.17	4.12E-04	2.17
	640	3.71E-06	2.00	2.38E-06	2.00	3.86E-04	2.07	9.79E-05	2.07

1D telegraph equation: discontinuity test

Let $\Omega_x = [-1, 1]$, $f_0(x, v) = \begin{cases} 1, & |x| \leq 0.2; \\ 0, & |x| > 0.2. \end{cases}$

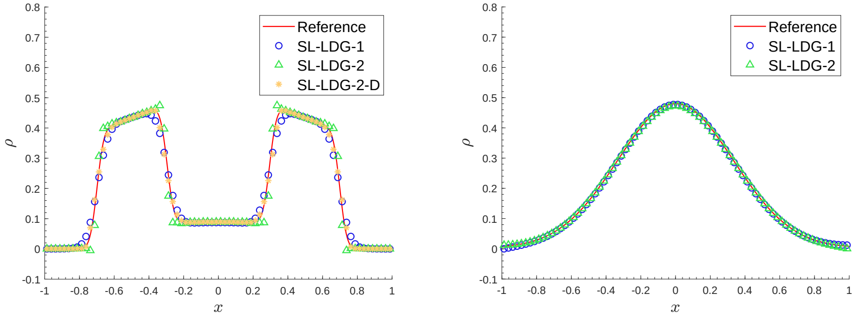

(a) kinetic regime: $\varepsilon = 1.0$, $T = 0.5$ (b) diffusive regime: $\varepsilon = 10^{-6}$, $T = 0.05$

Figure: Square wave problem for 1D telegraph equation. Density ρ of the SL-LDG-p ($p = 1, 2$) solutions at different regimes. $h = 0.025$ and $\Delta t = 1.5h$.

1D transport problem: isotropic Dirichlet BC

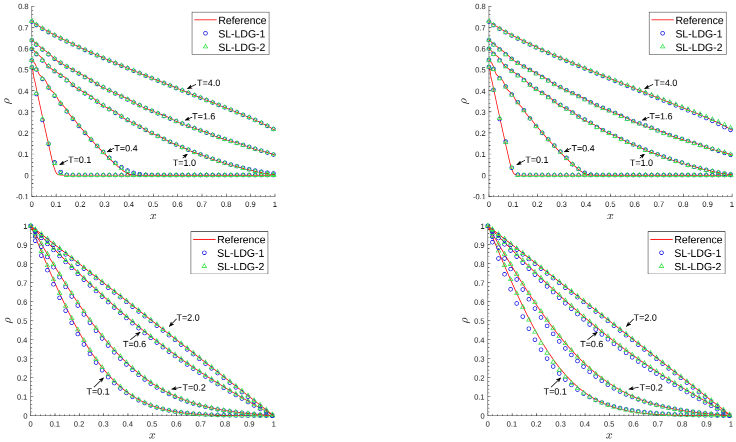

Figure: Isotropic Dirichlet boundary test for 1D transport problem. Density ρ of the SL-LDG-p ($p = 1, 2$) solutions at different regimes. $h = 0.0125$. Upper: $\varepsilon = 1.0$; Lower: $\varepsilon = 10^{-6}$; Left: $\Delta t = 0.5h$; Right: $\Delta t = 2.5h$.

2D transport problem: line source test

Let $\Omega_x = [-0.6, 0.6]^2$, $\varepsilon = 1$, $\sigma_s = 1$, $\sigma_a = S = 0$, $\zeta^2 = 3.2 \times 10^{-4}$.

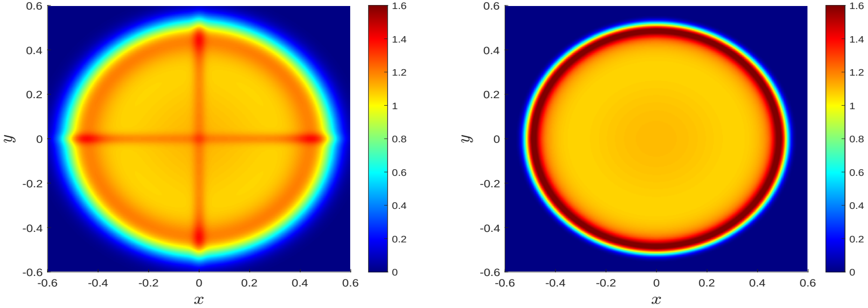

(a) SL1-LDG1, $\Delta t = 2.5h$

(b) SL2-LDG2, $\Delta t = 2.5h$

Figure: 2D Line source test. Density ρ of the SL-LDG-p ($p = 1, 2$) solutions at $T = 0.5$. $N_x = N_y = 128$, $N_v = 5810$.

2D transport problem: line source test

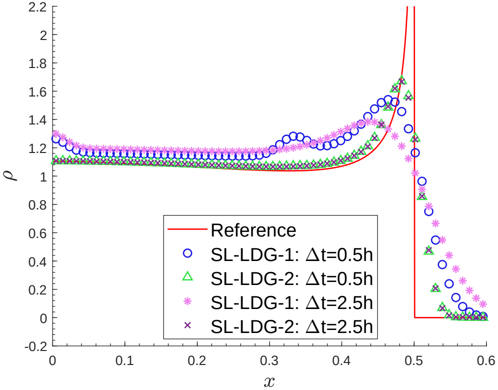

Figure: 2D Line source test. Slices at $y = 0$ of density ρ of the SL-LDG-p ($p = 1, 2$) solutions and a reference solution[5] at $T = 0.5$. $N_x = N_y = 128$, $N_v = 5810$.

[5] Bennett and McClarren 2022.

2D transport problem: varying scattering

Let $\Omega_x = [-1,1]^2$, $\varepsilon = 0.01$, $\sigma_a = S = 0$, $\zeta = 10^{-2}$,

$$\sigma_s(x,y) = \begin{cases} 0.999c^4(c+\sqrt{2})^2(c-\sqrt{2})^2 + 0.001, & c = \sqrt{x^2+y^2} < 1; \\ 1, & \text{otherwise.} \end{cases} \tag{42}$$

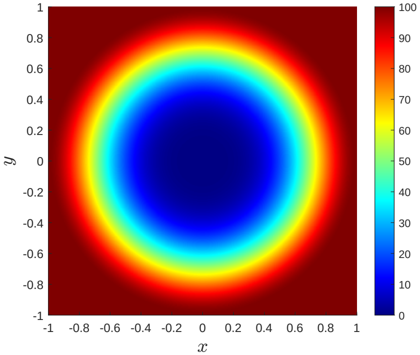

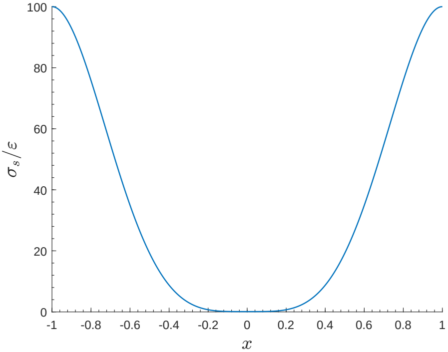

Figure: Plot of scattering coefficient σ_s/ε. Left: contour; Right: slice at $y = 0$.

2D transport problem: varying scattering

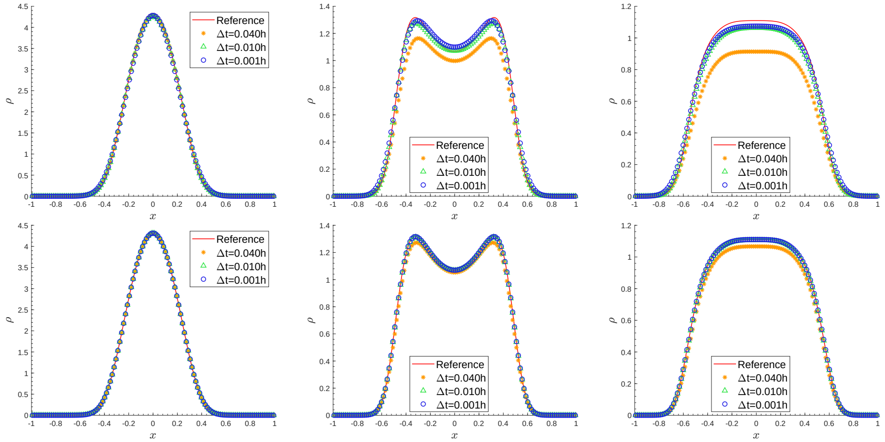

Figure: 2D Varying scattering problem. Density ρ at $y = 0$ of the SL-LDG-p ($p = 1, 2$) solutions with $N_x = N_y = 128, N_v = 590$. Upper: SL-LDG-1; Lower: SL-LDG-2; Left to Right: $T = 0.002, 0.006, 0.010$.

3D transport problem: varying scattering

Let $\Omega_x = [-1,1]^3$, $\Omega_v = \mathbb{S}^2$, $\varepsilon = 0.01$, $\sigma_a = S = 0$, $\zeta = 10^{-2}$,

$$\sigma_s(x,y,z) = \begin{cases} 0.999c^4(c+\sqrt{2})^2(c-\sqrt{2})^2 + 0.001, & c = \sqrt{x^2+y^2+z^2} < 1; \\ 1, & \text{otherwise.} \end{cases} \tag{43}$$

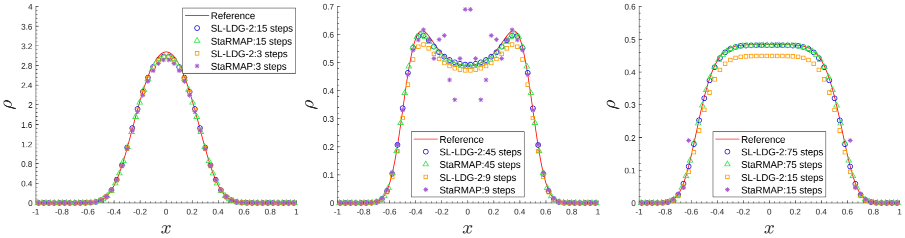

(a) $T = 0.002$ (b) $T = 0.006$ (c) $T = 0.010$

Figure: 3D Varying scattering problem. Comparison of the StaRMAP-P_{13} and SL-LDG-2-S_{194} solutions under different time steps. 1D density slices ρ at $y = z = 0$. $N_x = N_y = N_z = 50$.

3D transport problem: point source test

Let $\Omega_x = [-0.6, 0.6]^3$, $\varepsilon = 1$, $\sigma_s = 1$, $\sigma_a = S = 0$, $\zeta^2 = 3.2 \times 10^{-4}$.

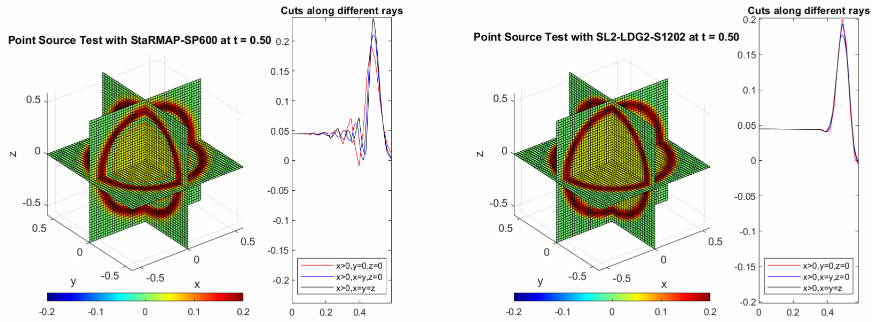

Figure: 3D Point source problem. Comparison of the StaRMAP[6] and SL-LDG-2 solutions. Animation. $N_x = N_y = N_z = 50$, $T = 0.5$ and $\Delta t = T/64$.

[6] Seibold and Frank 2014.

3D transport problem: point source test

Table: 3D Point source problem. Parallel efficiency of the SL-LDG-2 method. Parameters are $N_x = N_y = N_z = 50$, $N_v = 1202$, $T = 0.5$ and $\Delta t = 0.025$. P is the number of threads; RT is the running time; S is the speedup ratio; E is the parallel efficiency. The time unit is second.

P	RT_{total}	S_{total}	E_{total}	RT_ρ	S_ρ	E_ρ	RT_f	S_f	E_f
1	13552.66	-	-	8364.99	-	-	4163.34	-	-
2	6835.17	1.98	99.14%	3947.65	2.12	105.95%	2297.08	1.81	90.62%
4	3512.93	3.86	96.45%	1931.29	4.33	108.28%	1247.16	3.34	83.46%
8	1641.28	8.26	103.22%	764.02	10.95	136.86%	647.89	6.43	80.32%
16	1047.95	12.93	80.83%	466.11	17.95	112.17%	355.25	11.72	73.25%

Outline

Conclusion and future work

Conclusion:

- efficient first and second order AP SL DG methods for kinetic transport equation in a diffusive scaling;
- leverage the SL techniques in a weak form to enhance computational efficiency;
- uniformly unconditional stable in the linear scenario (Fourier analysis);
- oscillation-free damping approach for the SL DG scheme;
- pretty efficient for high-dimensional problems in varying regimes.

Future work:

- more general collision operators;
- frequency-dependent kinetic problems;
- rigorous energy stability analysis.

Reference:

- Y Cai, G Zhang, H Zhu and T Xiong, Asymptotic Preserving Semi-Lagrangian Discontinuous Galerkin Methods for Multiscale Kinetic Transport Equations, Journal of Computational Physics, 2024 (accepted)

Thank you for your attention!